OXIDATION IN A TEMPERATURE GRADIENT

G. R. Holcomb, B. S. Covino, Jr., and J. H. Russell
Materials Conservation Division
Albany Research Center
U.S. Department of Energy
Albany, OR 97321

ABSTRACT

The effects of a temperature gradient and heat flux on point defect diffusion in protective oxide scales were examined. Irreversible thermodynamics were used to expand Fick's first law of diffusion to include a heat flux term—a Soret effect. Oxidation kinetics were developed for the oxidation of cobalt and for nickel doped with chromium. Research in progress is described to verify the effects of a heat flux by oxidizing pure cobalt in a temperature gradient above 800°C, and comparing the kinetics to isothermal oxidation. The tests are being carried out in the new high temperature gaseous corrosion and corrosion/erosion facility at the Albany Research Center.

INTRODUCTION

Temperature gradients and high heat flux conditions abound in fossil energy generation systems. In coal-fired boilers, heat fluxes of 400 kW/m^2 are found in furnace section evaporator tube walls and 200 kW/m^2 in superheater tube walls.[1] Even greater heat fluxes are found in turbine blades. Oxidation and corrosion behavior in the presence of a temperature gradient can be different than in isothermal conditions. For example, thermal stresses can affect scale adhesion and point defect diffusion within oxide scales can be increased or decreased. The diffusion aspects of oxidation in a temperature gradient are addressed here.

The goals of this research are to understand the effects of temperature gradients and heat flux on oxidation for improved alloys and coatings, and to allow for better use of isothermal laboratory data as a predictor of actual service life.

The theoretical background for oxidation rate changes in high heat flux conditions will be presented for the oxidation of pure cobalt and for nickel doped with chromium. Experimental research in progress on the oxidation of pure cobalt in a temperature gradient will then be described. The new high temperature gaseous corrosion and corrosion/erosion facility will be described.

THEORY

Temperature gradients in a solid oxide result in two changes that modify diffusion within the oxide. The first is when equilibrium concentrations of point defects are a function of temperature. A gradient in point defect concentration can be created within the oxide, for example, in the case where more vacancies are expected at higher temperature. The second change is associated with the heat carried with each diffusion jump of an atom. Since each jump results in a transport of heat, the presence of a temperature gradient biases the jumps. This transport of heat is described by the heat of transport, Q^*, and is the heat carried from the initial site to the final site.[1]

---

[1] A similar term found in the literature is the reduced heat of transport, $Q^{*'}$, and is the portion of Q^* in excess of the partial molar enthalpy, h. Thus $Q^{*'} = Q^* - h$.

Both Glover[2] and Malik[3–4] have used non-equilibrium thermodynamics[5] to develop general flux equations that can be combined with point defect information of specific oxides to predict oxidation rates. The general flux equation, from Malik,[3–4] is

$$J_i = -\frac{Nc_i D_i}{kT}\left\{(1-t_i)\left[\frac{dm_i}{dx}+\frac{Q_i^* dT}{Tdx}\right]-q_i\sum_{k\neq i}\frac{t_k}{q_k}\left(\frac{dm_k}{dx}+\frac{Q_k^* dT}{Tdx}\right)\right\} \quad (1)$$

Where J_i is the flux of species i in the oxide, N is the number of lattice sites available to species i per unit volume, c_i is the concentration of species i, D_i is the diffusion coefficient of species i, k is Boltzmann's constant, T is temperature, t_i is the transport number of species i, $\grave{i}_i$ is the chemical potential of species i, x is the distance into the oxide from the metal, and q_i is the effective charge of species i. Equation 1 differs from Glover[2] by including the consequences of effective charge on the diffusion process (t_i and the q_i term). When the temperature gradient is zero and neglecting any effects of effective charge, then Eq. 1 simplifies to Fick's first law of diffusion.

To apply Eq. 1 to a particular system, details of the defect structure and transport must be available or assumed. CoO is a metal deficient ($Co_{1-y}O$), p-type semiconductor that is approximately stoichiometric when in equilibrium with cobalt metal.[6] The predominant point defects are cation vacancies, singly-charged (relative to the cobalt matrix) at moderate to high oxygen partial pressures (P_{O2}) and doubly-charged at low P_{O2}. Assuming that the predominant point defects are singly-charged vacancies, their formation can be described with Kröger-Vink notation by

$$\tfrac{1}{2}O_2 = V_{Co}^{'} + h^{\bullet} + O_O^x \quad (2)$$

Where V_{ω} is a singly-charged cobalt vacancy, $h^{\cdot}$ is an electron hole and O^x_O is an oxygen ion at an oxygen site. Using the law of mass action, the corresponding defect equilibrium is

$$\left[V_{Co}^{'}\right]p = K_{V_{Co}^{'}} P_{O_2}^{\frac{1}{2}} \quad (3)$$

Where p is the concentration of electron holes and $K_{V_{\omega}}$ is the equilibrium constant of Eq. 2. When impurities, intrinsic ionization, and minority defects are neglected, the simplified electrical neutrality condition becomes

$$\left[V_{Co}^{'}\right] = p = K_{V_{Co}^{'}}^{\frac{1}{2}} P_{O_2}^{\frac{1}{4}} \quad (4)$$

The mobility of electron holes is much larger than that of cobalt vacancies, so the approximation was made that $t_h \cdot = 1$ and $t_{V_{\omega}} = 0$. Other assumptions are that J_{Co} is constant at all points in the oxide scale, the temperature gradient is linear across the oxide scale, Q_i^* values are independent if temperature, $Q_h^* << Q_{V_{\omega}}^*$, and $Q_{V_{\omega}}^* = -Q_{Co}^*$. After these assumptions are made, the resulting expression is

$$J_{Co} = \frac{4kND_o(dT/dx)}{Q_{Co}^* + 2h_v}\left[\frac{\left[V_{Co}^{'}(x)\right]\exp\left(\frac{Q_{Co}^*}{2kT_x}\right)-\left[V_{Co}^{'}(0)\right]\exp\left(\frac{Q_{Co}^*}{2kT_0}\right)}{F(u_0)-F(u_x)}\right] \quad (5)$$

Where D_o is the frequency factor in the Arrhenius expression for vacancy diffusion ($D_{V\ co} = D_o \exp(-h_v/RT)$), h_v is the activation energy for vacancy diffusion, the x and 0 subscripts refer to the oxide-gas and metal-oxide interfaces. $F(u_i)$ is evaluated using

$$u_i = \frac{Q^*_{Co} + 2h_v}{2RT_i} \tag{6}$$

and

$$F(u) = -\frac{e^u}{u} + \ln|u| + u + \frac{u^2}{2\times 2!} + \frac{u^3}{3\times 3!} + \ldots + \textit{many terms for convergence} \tag{7}$$

After J_{Co} is known as a function of scale thickness, Eq. 5 can be integrated to obtain scale thickness as a function of time. The parameters used to find J_{Co} as a function of scale thickness are given in Table 1. The value of Q_{Co}^* is not known. Glover[2] approximated it with the activation energy for vacancy diffusion, h_v, and Malik[3–4] equated it with various multiples of h_v (e.g. –1, 0, 1, and 2). In Table 1, a representative value of 100 kJ/mol was used.

Table 1. Parameters used for oxidation of cobalt in a temperature gradient

Parameter	Value	Reference
D_o	0.02 cm^2/s	Koel and Gillings[7]
N	$5.18\cdot10^{22}$ sites/cm^3	Malik[3]
h_v	109 kJ/mol	Koel and Gillings[7]
$[V_{Co}(x)]$	$0.147\exp(-3925/T)P_{O2}^{1/4}$ vacancies/site	Koel and Gillings[7]
$[V_{Co}(0)]$	$0.147\exp(-4.252-17990/T)$ vacancies/site	Koel and Gillings[7] with Kubaschewski and Alcock[8] for $2CoO = 2Co+O_2$ equilibrium at the metal-oxide interface
Q_{Co}^*	100 kJ/mol	

Figure 1 shows some representative curves for both the isothermal (at 1050°C and 1000°C) and non-isothermal (with Q_{Co}^* values of 0 and 100 kJ/mol) oxidation of Co to CoO in air. For the integration of Eq. 5, boundary conditions were chosen such that T_0 and T_x maintained constant values of 1000°C and 1050°C. The "dT/dx, Q=0" curve shows the effects of a temperature gradient on oxidation kinetics from point defect concentrations and diffusion rates. The "dT/dx, Q=100 kJ/mol" shows how the heat of transport can decrease the oxidation rate. A negative heat of transport, as typical with interstitials, would increase the corrosion rate. Figure 1 shows the effects of a temperature gradient to be quite modest on the oxidation kinetics. However, the selection of boundary conditions makes a large difference in the effect. In Fig. 1, the heat flux and temperature gradient decrease with increasing scale thickness and time. When one temperature and the temperature gradient are fixed, then the resultant plots show a much larger effect.

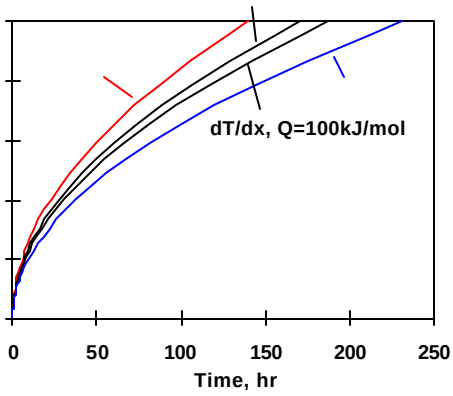

Fig. 1. Isothermal and non-isothermal oxidation of cobalt in air.

A similar treatment, based on Eq. 1, can be made for more complex systems. One example is nickel doped with chromium. Up to the solubility limit, where $NiCr_2O_4$ forms, trivalent chromium occupies divalent nickel sites, $Cr^{\cdot}_{Ni}$. Above 850°C, electrical neutrality is maintained with doubly charged nickel vacancies, V_{Ni}.[9] The formation of these defects is described by

$$NiCr_2O_4 = Ni^x_{Ni} + 2Cr^{\bullet}_{Ni} + 4O^x_O + V^{''}_{Ni} \tag{8}$$

where Ni^x_{Ni} is a nickel ion on a nickel site. The simplified electrical neutrality condition is

$$[Cr_{total}] = [Cr^{\bullet}_{Ni}] = 2[V^{''}_{Ni}] \tag{9}$$

Since the jump frequency of chromium ion-vacancy exchange is approximately one tenth of the jump frequency for nickel ion-vacancy exchange,[10] the transport number of V_{Ni} can be approximated[2] by 20/21 and of $Cr^{\cdot}_{Ni}$ by 1/21. Since the chromium solubility is low, J_{Ni} is approximately equal to $-J_{Vni}$. In a similar fashion as was done for Eq. 5, the resulting flux from Eq. 1 becomes

$$J_{Ni} = \frac{9kND_o(dT/dx)}{42(3h_v - Q^*_V - 2Q^*_{Cr})}\left[\frac{[C_{Co}(x)]\exp\left(-\frac{Q^*_V + 2Q^*_{Cr}}{3kT_x}\right) - [C_{Co}(0)]\exp\left(-\frac{Q^*_V + 2Q^*_{Cr}}{3kT_0}\right)}{F(u_0) - F(u_x)}\right] \tag{10}$$

where

$$u_i = \frac{3h_v - Q^*_V - 2Q^*_{Cr}}{3kT_i} \tag{11}$$

EXPERIMENTAL FACILITY

A new high temperature gaseous corrosion and corrosion/erosion facility was constructed at the Albany Research Center (ARC) to test materials for fossil energy applications in both oxidizing and reducing conditions. Within the facility are six small rooms, or modules, for conducting experiments. One module is shown in Fig. 2. Each module has access to CO, CO_2, H_2, CH_4, SO_2, HCl, H_2S, O_2, and N_2 gases from an adjoining gas shed located outside the building. As shown in Fig. 2, each gas within a module has an associated solenoid valve, a check valve, a digital mass flow controller (DMDC), and a flash arrester (where needed). Located outside each module are manual valves, and electrical switches

Fig. 2. Module with gas distribution system.

[2]The transport number is $D_iNq_i^2C_i/Ó(D_iNq_i^2C_i)$, so $t_V \approx 10\cdot 2^2\cdot 1/(10\cdot 2^2\cdot 1+1\cdot 1^2\cdot 2)=40/42=20/21$ and $t_{Cr}\approx 1/21$.

for solenoid valves and DMFCs for each gas. A control room, located adjacent to the lab, allows for analog and digital data collection and process control, and the setting of mass flow controllers.

Safety systems include gas detection monitors in each module, in the room containing the modules, and in the gas shed. Besides visual and audible alarms, relays are set to increase ventilation, to turn off gases at individual modules or at the gas shed, and to flush the gas lines with nitrogen. Personnel working in the facility are required to go through extensive safety and procedures training. Hazardous gas disposal includes neutralization traps for HCl, thermal oxidation for H_2S, H_2, CH_4, and CO, and activated carbon filtering for SO_2.

The focus areas for initial experiments for each module are

1. Oxidation in a temperature gradient
2. Hydrogen filter permeability
3. Corrosion under ash and salt deposits
4. Oxidation/sulfidation resistant materials
5. Erosion-corrosion
6. Refractory fluxing

OXIDATION OF COBALT IN A TEMPERATURE GRADIENT

In an attempt to verify the theory of oxidation in a temperature gradient, Malik[3–4] examined the oxidation of nickel at 600 to 900°C. The results were inconclusive. Besides the inherent difficulty in measuring what may be a small effect (depending upon the value of Q_{Ni}^*), there were other factors that could have masked the effect. One factor was that the defect structure of NiO is very dependant upon impurity levels, which are very hard to control. A second factor is that most of the temperature range was below 800°C, where grain boundary diffusion becomes more predominant than lattice diffusion. In the present investigation, cobalt oxidation above 800°C was selected because: (1) the defect structure of CoO is much less susceptible to impurity effects; (2) above 800°C lattice diffusion should predominate; and (3) cobalt oxidation has been the subject of much study, so most model parameters are known. Also, like NiO, CoO forms a dense and adherent scale, which is needed for the temperature cycling inherent in the periodic measurements of scale thickness. Figure 3 shows the temperature and oxygen partial pressure limits for the experiments. The oxygen partial pressure is below the level where duplex $CoO+Co_3O_4$ scales form,[6] so only CoO forms. The oxygen partial pressure is above the level where doubly charged cobalt vacancies, V''_{Co}, become an important point defect,[6] so the approximation of Eq. 3 is suitable. And the temperature is above 800°C, so lattice diffusion predominates.

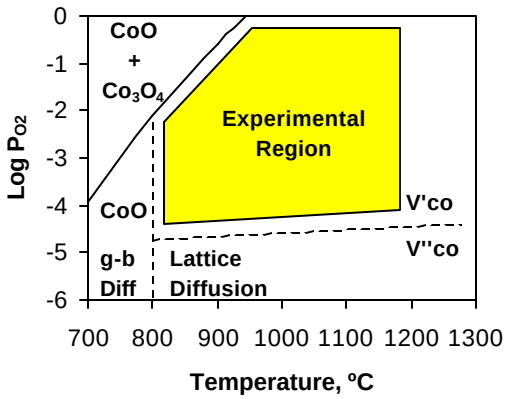

Fig. 3. Range of temperatures and oxygen partial pressures used in the oxidation of cobalt.

The overall experimental procedure closely follows the procedures that Malik[3–4] used. It consists of oxidizing one side of a piece of cobalt, while cooling the other side and measuring the temperature gradient across the sample. This establishes a known temperature gradient across the metal sample from which the heat flux is calculated using the thermal conductivity of cobalt. After exposure to oxygen at

temperature, the sample is removed from the furnace, the oxide scale nicked with a drill bit at a 45º angle, and the thickness of the scale measured with scanning electron microscopy (SEM) of the nick. The scale thickness, sample heat flux, sample temperature gradient, and CoO thermal conductivity are combined to calculate the temperature gradient across the oxide scale. The sample is then available for further oxidation.

A sample assembly is shown in Fig. 4. It consists of an inch diameter cobalt disk machined so that two thermocouples can be inserted and so that six small bolts can attach it to a stainless steel air-cooled chamber. The rest of the sample assembly is shown in Fig. 5, which is wrapped in insulation and inserted into a tube furnace, Fig. 6. The insulation wrap includes covering the outer circumference of the sample, to approximate one-dimensional heat flow within the sample.

Fig. 4. Sample assembly with a machined cobalt disk with internal thermal couples and attached to an air-

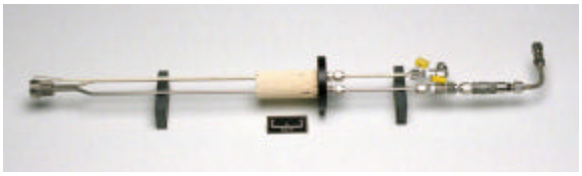

Fig. 5. Sample assembly for insertion into a tube furnace. Shown without insulation wrap.

An initial test was done with a sample temperature of approximately 950°C. A small heat flux was established across the sample of about 2.6 kW/m^2. When the gas in the furnace chamber was changed from pure nitrogen to an oxygen partial pressure of 0.1, the sample temperature rapidly increased to nearly 1100°C. This temperature response is shown in Fig. 7. The two temperature curves correspond to the two thermocouples within the sample. Evidently the heat of reaction for cobalt oxidation resulted in the rapid increase in temperature.

The oxide scale thickness was measured by nicking the surface at a 45º angle with a 0.040 inch (1 mm) diameter drill bit and examining the nick with SEM. Figure 8 shows both secondary electron (SE) and back-scattered electron (BSE) images of the nick, which is aligned 45º towards the top of the image. In this case, BSE best allows the scale thickness to be measured. It is equivalent to the width of the damaged scale above the exposed metal, and is 150 ± 20 ìm. This thickness is much larger than one would expect from isothermal parabolic kinetics. At 1100°C and a P_{O2} of 0.1, the isothermal parabolic rate constant[6] should be about 94 $mg^2/cm^4/hr$, which for 18 minutes predicts a scale thickness of 8.2 ìm.

There are several explanations that might account for the much larger scale thickness found in this test. First, there may be a leak or dead zone that allows for some oxygen to be present in the system during the gas purge. Second, initial oxidation kinetics could be much faster than the parabolic rate constant suggests. Third, it could be an effect of temperature gradients. Lastly, there could be some error in data collection or operating controls. The first explanation was examined by running a similar test on a new sample, but without any oxygen gas. After the same temperature ramp up to 950°C, the sample was held at temperature for 2 hours and then allowed to cool. The SEM analysis of the nick showed a very thin oxide scale with a thickness of 3.4 ± 0.8 ìm. So there could be a small dead zone or leak in the system, but not enough to account for the large scale thickness. The idea that initial oxidation kinetics could be much faster than the parabolic rate constant can be dismissed with the data from Mrowec and Przybylski.[11] For similar conditions, they show parabolic behavior for time durations above about

Fig. 6. Tube furnace and module for oxidation in a temperature gradient.

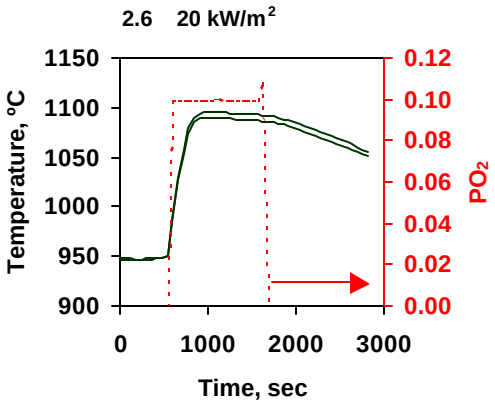

Fig. 7. Initial exposure of cobalt to oxygen and resulting temperature increase. The temperature curves are of both thermocouples within the sample.

2 minutes, and with data showing that the square of the mass change with time extrapolates back to zero at zero time. The third suggestion of temperature gradients seems suspect since most of the heat flux resulted from sample overheating after oxygen was introduced into the system. This would occur even in isothermal experiments without cooling of the back side of the sample. However, it could be that some initial oxidation is needed to prevent sample overheating with oxygen partial pressures as high as 0.1. Lastly, checks are underway of the data collection software and of process controls (such as the mass flow controllers).

SUMMARY

The presence of high heat fluxes and temperature gradients in many fossil energy systems creates the need for an understanding of their effects on corrosion and oxidation. Such information would be useful for both improved alloy design and for better translation of isothermal laboratory results to field use. The combined effects of temperature gradients on point defect concentration and mobility (heat of transport effects) are described with a theory of oxidation kinetics in a temperature gradient. Kinetic equations are developed for the oxidation of pure cobalt and of nickel doped with chromium. An attempt to verify the theory is currently in progress by examining the oxidation of cobalt, with the idea of future experiments in more complex and useful alloy systems. The experiments are taking place in ARC's new facility for high temperature gaseous corrosion and corrosion/erosion.

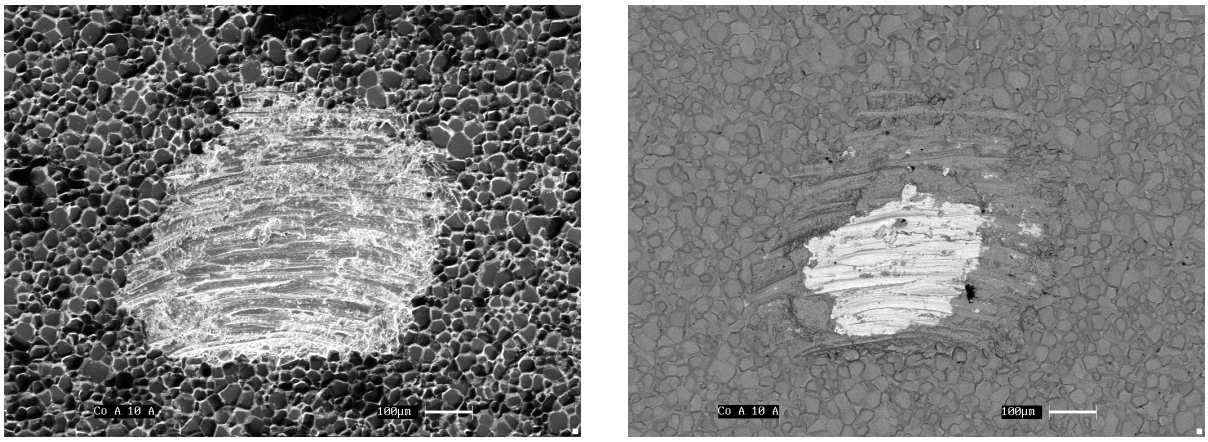

Fig. 8. Scanning electron microscopy of the CoO scale formed from the exposure to oxygen shown in Fig. 7 and nicked at a 45° angle. On the left is the secondary electron (SE) image showing the surface morphology. On the right is the back-scattered electron (BSE) image showing atomic weight information, so the lighter area is Co and the darker area is CoO. Scale thickness was measured using the middle portion of the damaged CoO part of the BSE image. Scale thickness is 150 ± 20 µm.

REFERENCES

1. J. B. Cutler and E. Raask, "External Corrosion in Coal-Fired Boilers: Assessment from Laboratory Data," Corrosion Science 21 (1981) pp. 789–800.
2. D. M. Glover, "Heat Flux Effects on Oxidation Rates and Kinetics," Corrosion Science 20 (1980) pp. 1185–1193.
3. S. Malik, "Oxidation of Metals in a Temperature Gradient," Ph.D. Thesis, University of Kent at Canterbury (1990).
4. S. Malik and A. V. Chadwick, "Oxidation in a Temperature Gradient," Microscopy of Oxidation, (Institute of Metals, 1991) pp. 336–341.
5. R. E. Howard and A. B. Lidiard, "Matter Transport in Solids," Reports on Progress in Physics 27 (1964) pp. 161–240.
6. P. Kofstad, *High Temperature Corrosion*, (Elsevier Applied Science, New York, 1988) pp. 93–100, 183–186.
7. J. Koel and P. J. Gillings, "The Contribution of Different Types of Point Defects to Diffusion in CoO and NiO During Oxidation of the Metals," Oxidation of Metals 5 (1972) pp. 185–203.
8. O. Kubaschewski and C. B. Alcock, *Metallurgical Thermochemistry*, 5th Ed, (Pergamon Press, New York, 1979) p. 379.
9. H. Meier and R. A. Rapp, "Electrical Conductivities of Pure NiO and Chromium-Doped NiO," Zeitschrift für Physikalische Chemie 54 (1971) pp. 168–189.
10. R. A. Perkins and R. A. Rapp, "The Concentration-Dependent Diffusion of Chromium in Nickel Oxide," Metallurgical Transactions 4 (1973) pp. 193–205.
11. S. Mrowec and K. Przybyski, "Oxidation of Cobalt at High Temperature," Oxidation of Metals 11 (1977) pp. 365–381.